

Preparation and Properties of Ethylene–Propylene–Diene Rubber/Organomontmorillonite Nanocomposites

Wei Li, Yu Dong Huang, and Seyed Javad Ahmadi

Polymer Materials and Engineering Division, Department of Applied Chemistry, Faculty of Science, Harbin Institute of Technology, Harbin 150001, People's Republic of China

Received 24 November 2003; accepted 11 March 2004

DOI 10.1002/app.20743

Published online in Wiley InterScience (www.interscience.wiley.com).

ABSTRACT: Ethylene–propylene–diene rubber (EPDM)/organomontmorillonite (OMMT) nanocomposites were prepared with a maleic anhydride grafted EPDM oligomer as a compatibilizer via melt intercalation. X-ray diffraction and transmission electron microscopy indicated that the silicate layers of OMMT were exfoliated and dispersed uniformly as a few monolayers in nanocomposites. The change in the crystallization behavior of the nanocomposites was examined. The nanocomposites exhibited great improvements in

the tensile strength and tensile modulus. The incorporation of OMMT gave rise to a considerable reduction of $\tan \delta$ and an increase in the storage modulus. Moreover, the solvent resistance of the nanocomposites increased remarkably. © 2004 Wiley Periodicals, Inc. *J Appl Polym Sci* 94: 440–445, 2004

Key words: clay; miscibility; nanocomposites; oligomers; rubber

INTRODUCTION

Recently, polymer nanocomposites containing layered silicates have attracted great interest from researchers because they frequently exhibit unexpected hybrid properties synergistically derived from two components.^{1,2} Montmorillonite (MMT) is a layered, mica-type clay mineral most commonly used in nanocomposite preparation. Its layered structure consists of two silica tetrahedral sheets and an edge-shared octahedral sheet of either aluminum or magnesium hydroxide. Stacking layers approximately 1 nm thick with a weak dipolar force leads to interlayers or galleries between the layers. The galleries are normally occupied by cations such as Na^+ , Ca^{2+} , and Mg^{2+} , with which it is easy to form organomontmorillonite (OMMT) by an alkylammonium ion-exchange reaction. OMMT can be either intercalated by macromolecules or exfoliated when they are dispersed in a polymer. Of all the methods used to prepare polymer/clay nanocomposites, the most versatile and environmentally benign approach is based on direct polymer melt intercalation. Until now, polymer/clay nanocomposites such as polystyrene,^{3,4} nylon 6,⁵ poly(ethylene oxide),⁶ polypropylene,^{7–10} polyethylene,¹¹ poly(ϵ -caprolactone),¹² silicone rubber,¹³ and poly(styrene-*b*-butadiene)¹⁴ have been prepared by melt intercalation.

Ethylene–propylene–diene rubber (EPDM) is an unsaturated polyolefin rubber with wide applications; it has been extensively used in making automotive tire sidewalls, cover stripe, wires, cables, hoses, belting, footwear, roofing barriers, and sporting goods. However, EPDM/clay nanocomposites cannot be prepared easily because they are hydrophobic and have poor miscibility with polar clay silicates, even when modified by long, nonpolar alkyl groups. Usukai et al.¹⁵ prepared EPDM/clay hybrids via a vulcanization process with some special vulcanization accelerators, and they concluded that the intercalation of the EPDM molecules into clay galleries occurred during the time of the mixing-roll and vulcanization process. Chang et al.¹⁶ treated sodium MMT first with octadecylammonium ions and then with a liquid low-molecular-weight EPDM and then mixed OMMT with EPDM via a simple melt-compounding process. Because of the expanded height and increased hydrophobicity of OMMT, the EPDM rubber chains could intercalate into the interlayer during the compounding process.

In this study, we prepared EPDM/OMMT nanocomposites with maleic anhydride grafted EPDM oligomer as a compatibilizer via melt intercalation, and we studied the dispersibility of the clays and some properties of the nanocomposites. EPDM had good miscibility with the oligomer, so the EPDM macromolecules could intercalate into the galleries of OMMT after the intercalation of the polar oligomer. Because EPDM and the oligomer molecules were crosslinked together in the vulcanization process, the addition of small parts of the oligomer did not affect the properties of the vulcanized rubber.

Correspondence to: Y. D. Huang (huangyd@hope.hit.edu.cn).

EXPERIMENTAL

Materials

Pure Na⁺-type MMT was kindly supplied by Kuniimine Industrial Co. with a cation capacity of 119 mequiv/100 g. Octadecylamine, purchased from Fluka Co., was used as an organic modifier of MMT. EPDM (J-3062E; 68.5–74.5 wt % ethylene) was supplied by Jilin Chemical Ind. Co., Ltd. Maleic anhydride modified EPDM oligomer (EPDM-g-MAH; 0.8 wt % maleic anhydride grafted) from Huzhou Genius Engineering Plastics Co., Ltd., was used. All the chemicals were used without further purification.

Preparation of organically modified MMT

OMMT was prepared via an ion-exchange reaction in water with alkylammonium. MMT (12 g) was dispersed into 600 mL of deionized hot water (80°C) with continuous stirring. Octadecylamine (4.8 g, 17.8 mmol) and concentrated HCl (1.8 mL) were dissolved in 400 mL of hot water. The mixture was poured into a hot MMT–water solution under vigorous stirring for 1 h. The precipitate was washed with deionized hot water until chloride anions were not detected with a 0.1 mol L⁻¹ AgNO₃ solution, and then it was dried in a vacuum oven at 80°C. OMMT was ground and screened with a 320-mesh sieve.

Preparation of the EPDM/OMMT nanocomposites

Pellets of EPDM, EPDM-g-MAH [20 parts per hundred parts of rubber (phr)], and different amounts of OMMT were melt-blended in a rheometer mixer (RM-200, Harbin University of Science and Technology, Harbin, China) for 15 min at 90 rpm and 150°C. The obtained mixture, zinc oxide (5 phr), stearic acid (1 phr), vulcanization accelerator 2-mercaptobenzothiazole (0.5 phr), vulcanization accelerator tetramethylthiuram disulfide (TMTD; 1.5 phr), and sulfur (1.5 phr) were compounded with a mixing roll. Vulcanized EPDM was press-molded at 160°C for 20 min to obtain rubber sheets (250 mm × 150 mm × 2 mm). The nanocomposite containing 2 phr OMMT was abbreviated EONC2, and the nanocomposites with 5, 8, 10, and 15 phr OMMT were abbreviated EONC5, EONC8, EONC10, and EONC15, respectively. The sample without clay was named EO.

For comparison, conventional composites were prepared with pristine MMT with the aforementioned procedure. The conventional composites were labeled EOCC.

Measurements

X-ray diffraction (XRD) patterns were obtained with an X-ray diffractometer (X'Pert, Philips) equipped

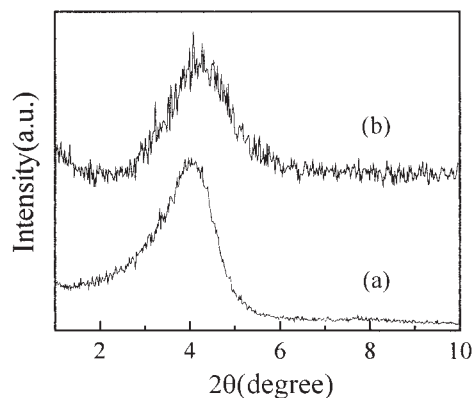


Figure 1 XRD patterns of (a) OMMT and (b) a mixture of EPDM and OMMT (6.25 wt %).

with Cu K α radiation at a generator voltage of 40 kV and a generator current of 40 mA. Diffraction data were collected for each interval of 0.02° between 1 and 10°.

Transmission electron microscopy (TEM) micrographs were obtained with a transmission electron microscope (H-800, Hitachi) at an accelerator voltage of 200 kV.

Tensile testing was performed with a universal testing machine (DCS-5000, Shimadzu) at an extension rate of 500 mm/min at room temperature according to China Industry Standard GB/T 528-92.

The dynamic mechanical properties were performed with a dynamic mechanical analyzer (DMTA V, Rheometric Scientific). The testing was carried out with a single-cantilever bending model at a frequency of 1 Hz and a heating rate of 2°C/min. The strain amplitude was 0.05% in the range of -100 to -20°C and 0.2% in the range of -20 to 100°C.

The solvent resistance was determined with a simple experiment. The test specimens were cut (20 mm × 10 mm × 2 mm). They were placed in a vacuum oven at 60°C for 24 h, were cooled in a desiccator, and immediately weighed to the nearest 0.001 g to obtain the initial weight (W_0). The conditioned specimens were entirely immersed in a container of xylene kept at $25 \pm 0.2^\circ\text{C}$ for 8 h. After 8 h, the specimens were removed from xylene, one at a time; the surface solvent on the specimens was removed with a dry cloth, and the specimens were weighed immediately to obtain the final weight (W_1). The percentage increase in the weight of the samples was calculated to the nearest 0.01% with the following formula: $(W_1 - W_0)/W_0$.

RESULTS AND DISCUSSION

XRD patterns

The XRD patterns of OMMT and a mixture of OMMT with EPDM are shown in Figure 1. OMMT has a

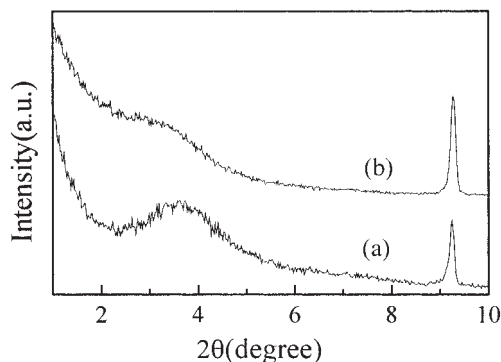


Figure 2 XRD patterns of (a) EPDM-g-MAH/OMMT (EPDM-g-MAH:OMMT = 3:1 w/w) and (b) a mixture of EPDM-g-MAH/OMMT and EPDM (EPDM:EPDM-g-MAH/OMMT = 3:1 w/w).

characteristic diffraction peak corresponding to the (001) plane at $2\theta = 4.0^\circ$, and the mixture also shows a peak at the same angle. This result means that EPDM molecules cannot intercalate into the galleries of OMMT by direct melt compounding. Like other polyolefin polymers, EPDM does not include any polar groups in its backbone, and the silicate layers of clay, even modified by long, nonpolar alkyl groups, are polar and incompatible with polyolefins.

Figure 2 shows the XRD patterns of EPDM-g-MAH/OMMT (the oligomer has an obvious diffraction peak at $2\theta = 9.1^\circ$ by itself) and a mixture of EPDM-g-MAH/OMMT and EPDM. The diffraction peak of EPDM-g-MAH/OMMT appears at a lower angle than that of OMMT, and this indicates that the polar oligomer can intercalate into the galleries of OMMT. Furthermore, the mixture shows the diffraction angle at a lower position than EPDM-g-MAH/OMMT. This clearly indicates that the matrix EPDM rubber chains can intercalate into the galleries of OMMT after the intercalation of the oligomer because of the good miscibility between the oligomer and EPDM.

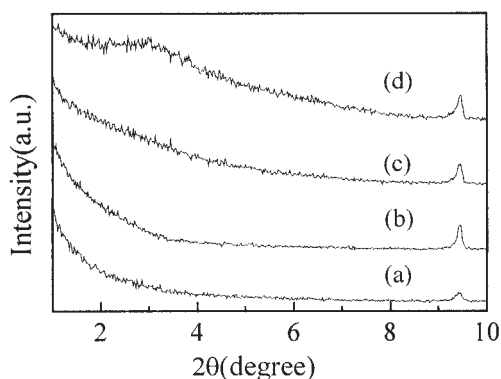


Figure 3 XRD patterns of unvulcanized nanocomposites: (a) EONC5, (b) EONC8, (c) EONC10, and (d) EONC15.

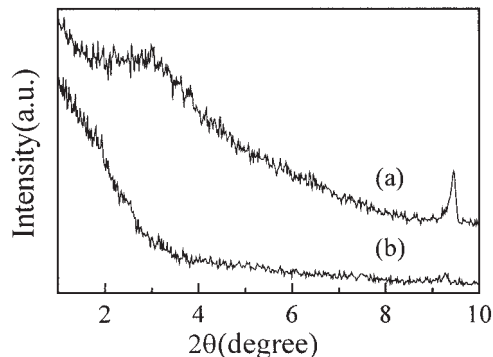


Figure 4 XRD patterns of (a) unvulcanized and (b) vulcanized EONC15.

Figure 3 shows the XRD patterns of unvulcanized nanocomposites. No diffraction peak of OMMT are shown when the OMMT loading is less than 10 phr, and this indicates that OMMT is exfoliated and dispersed at the molecular level into the rubber matrix. Although there is also a wide weak peak at a low angle when the OMMT loading is 15 phr, this peak disappears after vulcanization (Fig. 4). This result shows that the interlayer space of OMMT is further enlarged and then exfoliated during the vulcanization process. The mechanism is the same as that proved by Usukai et al.¹⁵ The vulcanization accelerator TMTD $\{[(\text{CH}_3)_2\text{NC}(\text{S})]_2\text{S}_2\}$ dissociates into radicals when the temperature is raised. The radicals combine with carbon atoms in EPDM chains to polarize EPDM molecules. These EPDM molecules intercalate into the clay galleries through hydrogen bonds between the polar EPDM and the clay surface.

The XRD patterns of vulcanized EOCC are shown in Figure 5. The diffraction peaks of EOCC appear at the same angle ($2\theta = 7.1^\circ$) as pristine MMT, and this indicates that the structure of MMT does not change in the conventional composites. EOCC has another sharp crystalline diffraction peak at $2\theta = 6.6^\circ$, which can also be seen for pure EPDM and EO (Fig. 6). The rubber

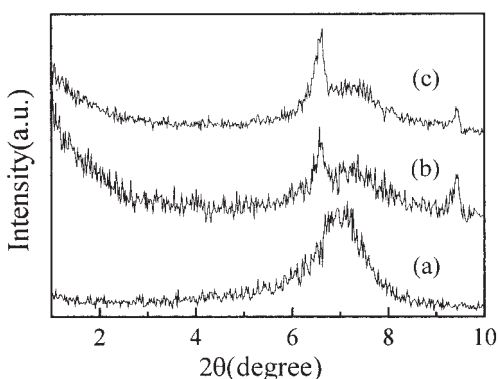


Figure 5 XRD patterns of (a) pristine MMT, (b) vulcanized EOCC10, and (c) vulcanized EOCC30.

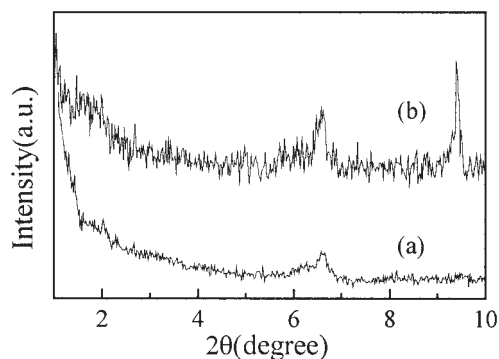


Figure 6 XRD patterns of two vulcanizates: (a) pure EPDM and (b) EO.

matrices exhibit crystalline diffraction peaks because the high content of ethylene in EPDM causes rubber crystallization. However, the vulcanized nanocomposites do not exhibit a crystalline diffraction peak (Fig. 4). It can be concluded that the strong interaction between the OMMT layers and the polymer molecules changes the crystallization behavior of the nanocomposites. Because macromolecules are only conventionally compounded with silicate layers in conventional composites, the crystallization behavior of rubber shows no difference with respect to EO and pure EPDM.

TEM observations

The clay dispersion was also observed with TEM. TEM can provide information about the spatial distribution and structure changes of silicate layers in real space. TEM images of EONC5 are shown in Figure 7(a); the dark lines are the cross sections of silicate layers 1 nm thick. The OMMT silicate layers are exfoliated and dispersed uniformly in the nanocomposite as a few monolayers, and this is compatible with the XRD results. These observations reveal that there is a certain strong interaction between OMMT and the rubber matrix. In a conventional composite [Fig. 7(b)], pristine MMT exists in major aggregates, and the silicate layers still maintain ordered stacking, whereas the layer distances are not almost changed; this indicates that the compatibility between pristine MMT and the rubber matrix is poor.

Tensile properties

The tensile properties of the nanocomposites and conventional composites have been measured and are summarized in Figure 8. The tensile strength and tensile modulus of the nanocomposites are substantially increased with respect to those of the conventional composites. The tensile strength of the nanocomposites increases rapidly with increasing OMMT content

from 0 to 5 phr and then decreases slowly when the OMMT content increases beyond 5 phr. EONC5 has a tensile strength of 12.01 MPa; a 158% improvement in the tensile strength is obtained in EONC5 with respect to EO. There is a significant improvement in the tensile modulus with increased clay content; the maximum improvement obtained in EONC15 is 97.1%. The enhancement in the tensile properties is attributed to the nanometric dispersion of silicate layers in the rubber matrix. The reduction of the tensile strength above the 5 phr OMMT loading is attributable to the inevitable slight aggregation of the layers with a high clay content.

Dynamical mechanical analysis

Figure 9 shows the effect of the type of fillers on $\tan \delta$ and the storage modulus of the composites as a function of the temperature. Figure 9(a) shows that the addition of MMTs results in a shift in T_g (the temperature at the peak of $\tan \delta$) toward a higher temperature. Although the T_g values of EOCC5 and EONC5 are almost the same, the peak value of $\tan \delta$ of the nanocomposites decreases slightly in comparison with that of EO. Moreover, there is a significant decrease in the $\tan \delta$ value of EONC5 above -10°C . These observations are ascribed to strong interfacial action be-

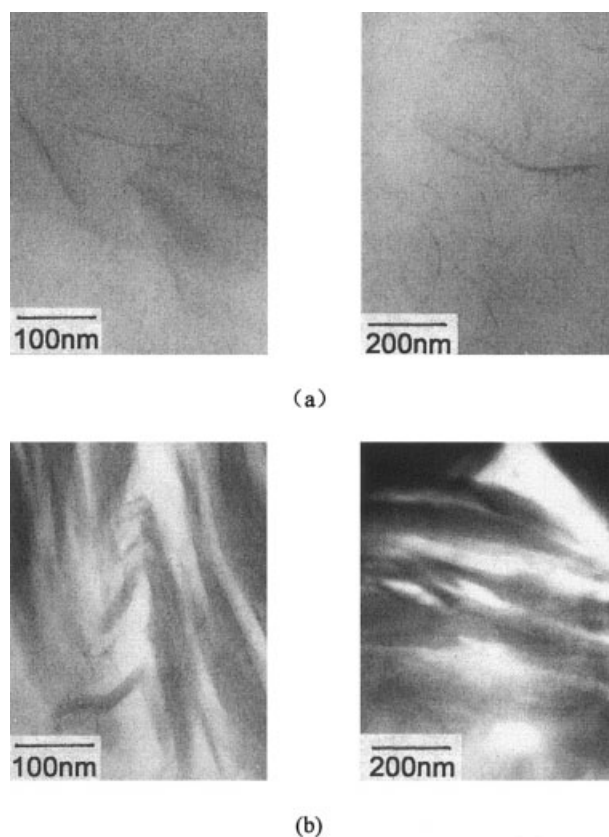
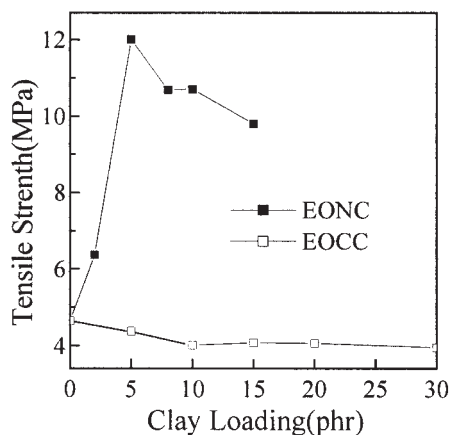
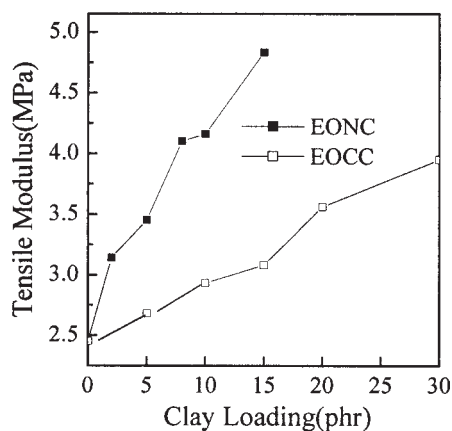


Figure 7 TEM images of (a) EONC5 and (b) EOCC5.



(a)



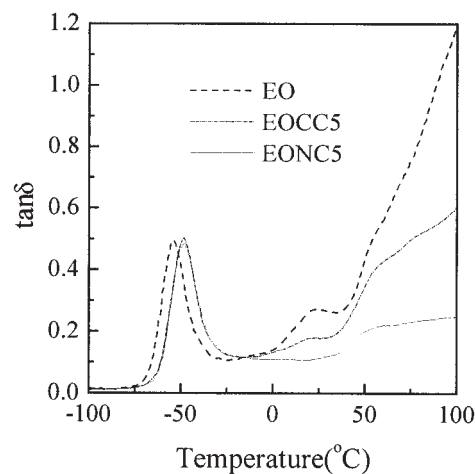
(b)

Figure 8 Effect of the clay loading on (a) the tensile strength and (b) the tensile modulus.

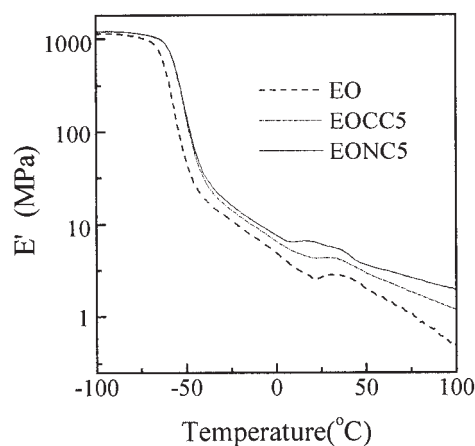
tween the rubber matrix and OMMT. Figure 9(b) shows that the storage modulus of EONC5 is larger than that of EOCC5 because of the greater reinforcing effect of OMMT.

Solvent resistance

The solvent resistance of the vulcanizates can be evaluated by the xylene adsorption because xylene is a good solvent of EPDM. The xylene adsorption results obtained with the previous formula are given in Table I. The xylene adsorption of EONC5 decreases 49.81% with respect to EO, whereas the xylene adsorption of EOCC5 decreases only 2.390%. This phenomenon can be explained by the fact that the OMMT layers, being dispersed on a nanometer scale in the polymer matrix, can enhance the mean free path of xylene molecules to pass more difficult through the networks of nanocomposites than through the pure rubber, whereas it is easy for xylene molecules to go around major pristine



(a)



(b)

Figure 9 Dynamic mechanical spectra: (a) $\tan \delta$ and (b) the storage modulus (E') as functions of the temperature for EO, EOCC5, and EONC5.

MMT aggregates and to pass through the conventional composites.

CONCLUSIONS

EPDM/OMMT nanocomposites were prepared successfully with a maleic anhydride grafted EPDM oligomer as a compatibilizer via simple melt intercalation. According to XRD and TEM analysis, the nanocomposites were exfoliated. The crystallization

TABLE I
Xylene Adsorption of the Vulcanizates

Vulcanizate	Xylene adsorption (%)
EO	359.8
EONC5	180.6
EOCC5	351.2

behavior of the nanocomposites changed because of the strong interaction between the OMMT layers and the polymer molecules. The tensile strength and tensile modulus of the nanocomposites were improved by the addition of OMMT. The incorporation of OMMT also gave rise to a considerable reduction of the $\tan \delta$ value and an increase in the storage modulus, which demonstrated the reinforcing effect of OMMT on the rubber matrix. The dispersion of OMMT nanolayers in the nanocomposites led to improved solvent resistance.

References

1. Alexandre, M.; Dubois, P. *Mater Sci Eng* 2000, 28, 1.
2. Lebaron, P. C.; Wang, Z.; Pinnavaia, T. J. *Appl Clay Sci* 1999, 15, 11.
3. Vaia, R. A.; Ishii, H.; Giannelis, E. P. *Chem Mater* 1993, 5, 1694.
4. Vaia, R. A.; Giannelis, E. P. *Macromolecules* 1997, 30, 8000.
5. Liu, L. M.; Qi, Z. N.; Zhu, X. G. *J Appl Polym Sci* 1999, 71, 1133.
6. Vaia, R. A.; Vasudevan, S.; Krawiec, W.; Scanlon, L. G.; Giannelis, E. P. *Adv Mater* 1995, 7, 154.
7. Kato, M.; Usukai, A.; Okada, A. *J Appl Polym Sci* 1997, 66, 1781.
8. Kawasumi, M.; Hasegawa, N.; Kato, M.; Usuki, A.; Okada, A. *Macromolecules* 1997, 30, 6333.
9. Hasegawa, N.; Kawasumi, M.; Kato, M.; Usuki, A.; Okada, A. *J Appl Polym Sci* 1998, 67, 87.
10. Hasegawa, N.; Okamoto, H.; Kato, M.; Usuki, A. *J Appl Polym Sci* 2000, 78, 1918.
11. Wang, K. H.; Choi, M. H.; Koo, C. M.; Choi, Y. S.; Chung, I. J. *Polymer* 2001, 42, 9819.
12. Lepoittevin, B.; Devalckenaere, M.; Pantousier, N.; Alexandre, M.; Kubies, D.; Calberg, C.; Jérôme, R.; Dubois, P. *Polymer* 2002, 43, 4017.
13. Wang, S. J.; Long, C. F.; Wang, X. Y.; Li, Q.; Qi, Z. N. *J Appl Polym Sci* 1998, 69, 1557.
14. Laus, M.; Francescangeli, O.; Sandrolini, F. *J Mater Res* 1997, 12, 3134.
15. Usukai, A.; Tukigase, A.; Kato, M. *Polymer* 2002, 43, 2185.
16. Chang, Y.-W.; Yang, Y. C.; Ryu, S. H.; Nah, C. W. *Polym Int* 2002, 51, 319.